Increased Understanding of
Neoclassical Internal Transport Barrier on CHS

T.Minami, A.Fujisawa, H.Iguchi, Y.Liang, K.Ida, S.Nishimura, M.Yokoyama, S.Murakami, Y.Yoshimura, M.Isobe, C.Suzuki, I.Nomura, K.Toi, M.Yoshinuma, A.Shimizu, C.Takahashi, K.Matsuoka, S.Okamura, CHS group

National Institute for Fusion Science, 322-6 Oroshi, Toki, 509-5292, Japan
E-mail: minami@nifs.ac.jp

Abstract.

We report the recent progress of the study on neoclassical internal transport barrier (N-ITB) on Compact Helical System experiment. N-ITB has been observed for EC heated NBI plasma. The improved confinement region for electrons is expanded compared to that of the previous N-ITB plasma heated by only ECH. Moreover, the ion temperature is found to be increased simultaneously by about two to three times ($T_i(0)\sim400$-500eV) with steep gradient region at $\rho\sim0.6$. From the measurement of the averaged peak energy intensity using the soft X-ray CCD camera it is confirmed that the impurity confinement is also improved with N-ITB. The radial electric field is observed to bifurcate into electron root ($E_r\sim15$kV/m) and rather large electric field shear ($dE_r/dr\sim300$kV/m^2) is produced in the layer between ion and electron root.

1. Introduction

The internal transport barrier of the helical devices plays an important role on plasma confinement like tokamaks. The barrier of the helical device is formed due to the positive electric field and the electric field shear. The radial electric field is determined by the ambipolar diffusion of neoclassical particle fluxes, so that this internal transport barrier is called neoclassical internal transport barrier (N-ITB).

In the previous N-ITB experiment on Compact Helical System (CHS) with the electron cyclotron heating plasma (ECH), the electron temperature increased up to ~3keV in the plasma core and the large temperature gradient ($dT_e/dr\sim43$ keV/m) was observed at the barrier point ($\rho\sim0.3$). This plasma is characterized by the large electric field ($E_r\sim7$kV/m) and the electric field shear ($dE_r/dr\sim-500$ kV/m^2). The drop of the electron thermal diffusivity to the level of the neoclassical transport ($\chi_e\sim2$-6 m^2/s) and the reduction of the density fluctuation (the reduction of the fluctuation power is 48%) were observed at the barrier location [1,2].

Recently N-ITB was also observed for EC heated NBI plasma [3]. The ion temperature increased as well as the electron temperature. In this paper, experimental observations of the new N-ITB plasma are reported and the transport properties are discussed.

2. Experimental Setup

CHS is a medium size heliotron/torsatron device with a poloidal mode number l=2 and a toroidal mode number m=8. The plasma major radius and averaged minor radii are 1.0 and 0.2m, respectively. The profiles of the electron and ion temperature are measured by the YAG Thomson scattering system and charge exchange spectroscopy (CXS). The YAG Thomson system has 24 spatial channels, spatial resolution is about 1-2 cm ,and repetition time of the measurement is 5-10 ms [4]. For low density plasma, we accumulate signals of several shots to obtain good S/N ratio (typical case 5-10). The CXS measurement using fully stripped carbon has 30 spatial points and the resolution is about 1 cm [5]. The charge exchange signal is accumulated for 20 ms and, for low density plasma, signal for 5-10 shots are summed up. Electron density profile and line averaged density are measured with the YAG Thomson system and the microwave interferometer. The radial electric field is measured by Heavy Ion Beam Probe (HIBP) of which the sample volume is a few cm. To investigate the impurity transport the photon counting two-dimensional
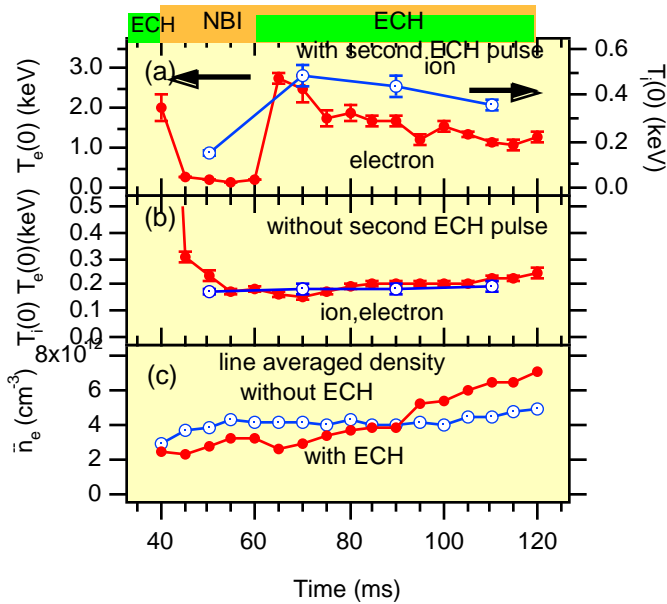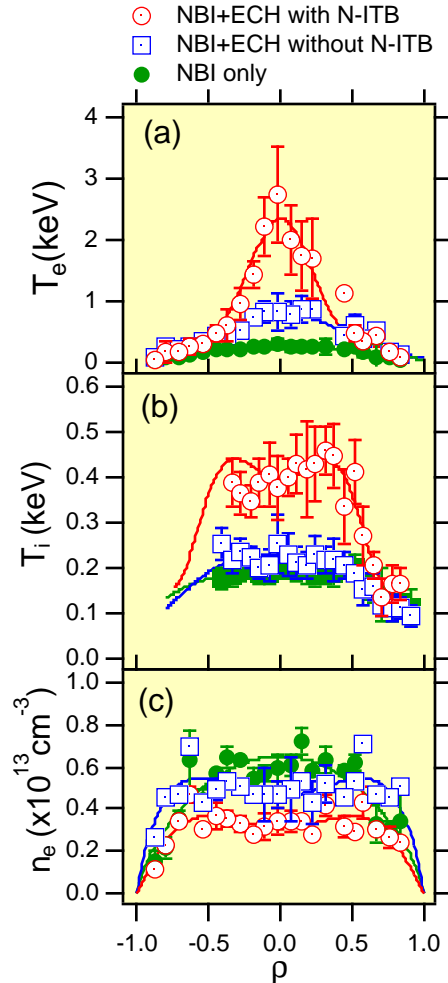
Figure 1. Time evolution of the typical EC heated NBI discharge with N-ITB (a) electron (red) and ion temperature (blue) with N-ITB (b) without second pulse of ECH (c) line averaged densities for two cases.

Figure 2. Radial profiles of the EC heated NBI plasma with N-ITB. (a) electron temperature (Te). (b) ion temperature (Ti.) (c) electron density (ne). The red circles denote with N-ITB. The blue squares denote without N-ITB. The green triangles denote without ECH.

x-ray CCD camera [1024x512 pixels] is used [6].

3. Simultaneous Increase of Electron and Ion Temperature in N-ITB Discharge

Figure 1 shows the typical time evolution of the central electron and ion temperature and the line averaged density for the N-ITB discharge (and NBI discharge without second pulse ECH as a reference). The target plasma is produced by the first pulse of 53.2GHz 2nd harmonic ECH ($P_{inj} \sim 130$-150kW, 20-40 ms), then heated and sustained by the NBI ($P_{inj} \sim 0.7$MW). The NBI is tangentially injected into the plasma. The magnetic field is 0.88T and the magnetic axis of the plasma is 92.1 cm. When the second pulse of ECH is superposed to the NBI plasma (60-120 ms), with the condition that density is below the critical value, the electron temperature increases up to ~3 keV with a sharp temperature gradient (Fig. 1 (a)). As the electron density gradually increases (Fig. 1 (c), red curve), the central electron temperature decreases to ~1 keV, which is one-third of that with N-ITB ,and the sharp temperature gradient disappears. These characteristics are generally similar to the results of the previous N-ITB ECH experiment without NBI. However, the significant difference is in the electron temperature profile: the improved confinement region is expanded in the present experiment and the temperature profile has "bell" shape rather than "dome" shape which was observed in the previous experiment.

Figure 2 (a) shows the electron temperature profile of N-ITB plasma. It also shows profiles of EC heated NBI plasma without N-ITB (density is above threshold) and NBI plasma without ECH. For N-ITB plasma, the foot point of the enhanced region of the electron temperature is located at
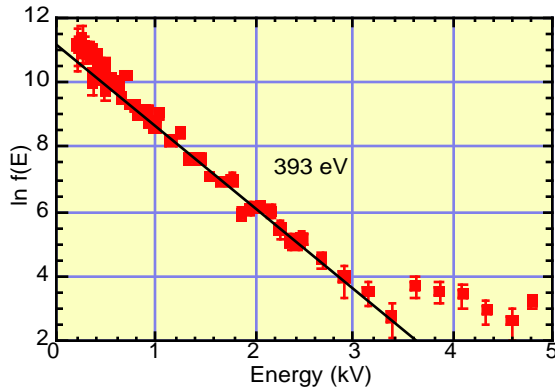
Figure 3. NPA spectrum in the EC heated NBI plasma with N-ITB. The fitting line show that the ion temperature is ~400 eV.
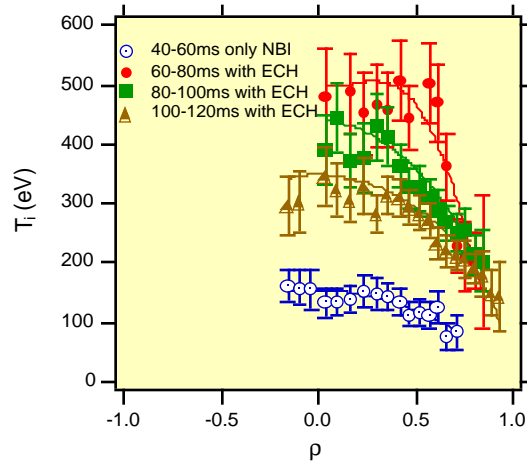
Figure 4. Time evolution of the ion temperature profile in the EC heated NBI plasma with N-ITB. The open circles and squares denote NBI phase in 40-60ms, and 100-120ms. The closed circles and squares denote ECH+NBI phase in 60-80, and 80-100 ms.

the outer location (ρ_f =0.4-0.5) compared to the previous ECH N-ITB experiment (ρ_f =0.3-0.4) [1,2,3]. The ion temperature simultaneously increases ($T_i(0)$~400-500 eV) by two to three times compared to the plasma without N-ITB. It is clearly different from the ion temperature (150-200 eV) of the NBI plasma without N-ITB. The sharp ion temperature gradient is also produced (8-12 keV/m) at the location ρ_g~0.4-0.7. The foot point for ion appears at outer position (ρ_f~0.7) than that for electrons. The neutral particle analyzer (NPA) is also used for ion temperature measurement. Figure 3 shows the spectrum of the NPA for the EC heated NBI plasma with N-ITB. The ion temperature is about 400 eV, which is in a good agreement with the result of CXS measurement.

Figure 1 (a) shows that the ion temperature slowly goes down as the density increase. Figure 4 shows the temporal evolution of the ion temperature profile. With second pulse of ECH, the ion temperature gradient grows up and the sharp shoulder of the temperature profile is produced. When the averaged density exceeds the threshold for N-ITB at 80 ms, the ion temperature gradient quickly decreases and the shoulder disappears. However decrease in the central ion temperature is relatively slow. After ECH is turned off, the ion temperature still remains around 400eV in spite of the density increase to $4\text{-}5\times10^{12}\text{cm}^{-3}$, which is above the threshold. In this period, the density profile is almost flat, thus the mechanism for the high ion temperature is not the same as the high T_i mode [7], because the High T_i mode is caused by the density peaking.

4. Critical Density for N-ITB Formation

The N-ITB formation strongly depends on the plasma density. Figure 5 (a) (b) shows the dependence of the central electron temperature and the temperature gradient at the N-ITB on the averaged density. When the averaged electron density is below the threshold density (n_e ~$4\times10^{12}\text{cm}^{-3}$), the central electron temperature considerably increases. The electron temperature gradient also increases to 20-30 keV/m). The threshold density and other characteristics are very close to the ECH plasma N-ITB experiments [8].

The dependence of the ion temperature on the density is the same as the electron temperature. As shown in Figure 5 (c), the central ion temperature rapidly increases by the application of ECH when the density is lower than $4\times10^{12}\text{cm}^{-3}$. On the other hand, when the averaged density is above the threshold, the ion temperature of the EC heated NBI plasma is almost the same as the NBI plasma without ECH. The ion temperature gradient increases from 2-3 keV/m up to 8-12 keV/m
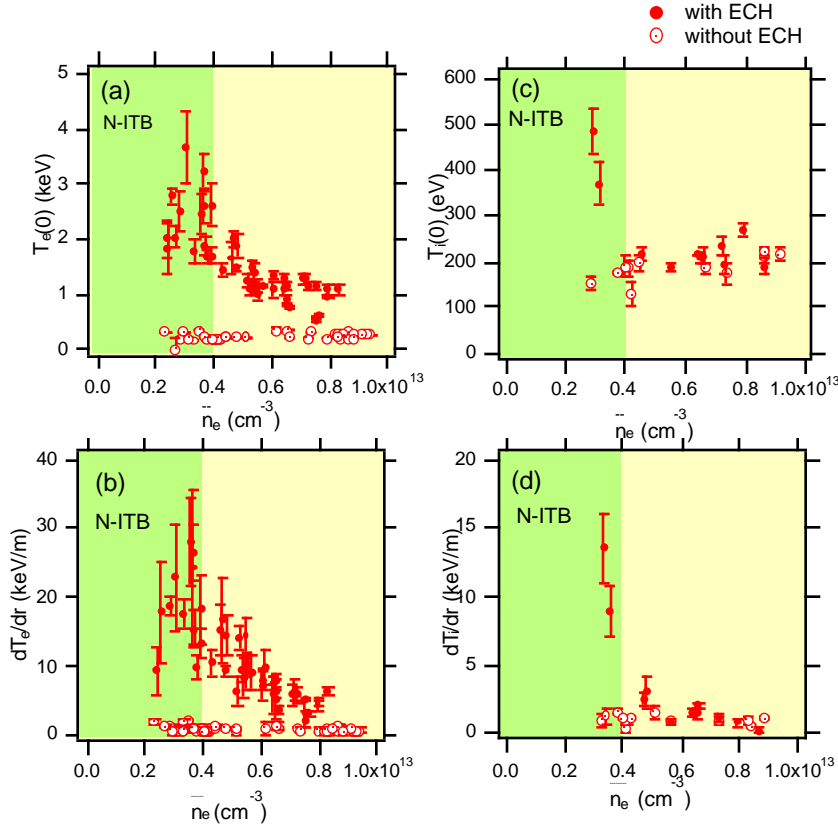
Figure 5. Central electron (a) and ion (c) temperature and electron temperature gradient (b) and ion temperature gradient (d) as a function of line averaged density. The close circles denote the plasam with ECH. The open circles denote the plasma without ECH.

in the case of N-ITB, while the gradient is comparable to that of the NBI plasma without ECH when the density is above the threshold.

5. Impurity Transport for N-ITB Plasma

It is important to study the particle transport in N-ITB plasma. As a part of such a study, the titanium impurity transport was measured with the soft X-ray CCD camera for the plasma with N-ITB. The CCD camera has an 900μm-thick Be filter and a pinhole of 0.3 mm-diameter. The energy resolution is 3.22 ± 0.04 eV/electron (16.5 ± 0.2eV/ADC count). Because the frame rate is slow (0.2Hz), all emission from the discharge in CHS (100-150 ms) is accumulated. The ionization level of the impurity ions are determined by the balance between the particle confinement and ionization. The energy level of T_i Kα lines depends on the charge state. Because the energy resolution of the soft X-ray camera is not enough to distinguish individual Kα lines for different charge states, we tried to measure the change of the charge states distribution from the shift of averaged energy of the Ti Kα lines.

Figure 6 (a) shows the energy spectra measured with X-ray CCD camera in EC heated NBI plasma experiments. For the plasma with N-ITB, the peak energy of the intensity of Ti Kα line at ρ=0.03 is 4.72-4.73 keV which is dominated by He-like ions. For the plasma without N-ITB, the peak energy is shifted to 4.68-4.69kV which is dominated by Be-like ions [6]. The averaged peak energy depends on the electron temperature and the diffusivity of the impurity. To evaluate the diffusion coefficients of impurity in the plasma, the numerical impurity code MIST and LINES are used.
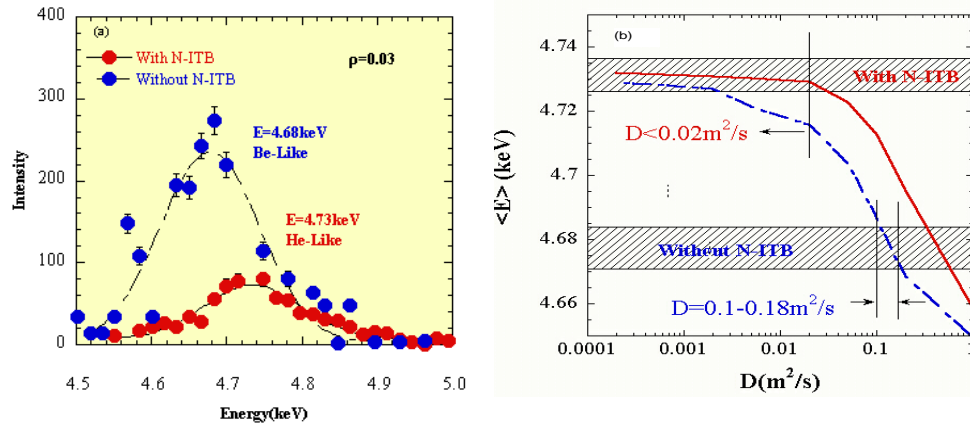
Figure 6. (a) Energy spectrum for the plasmas with and without N-ITB. (b) The calculated averaged energy of the Ti spectrums as a function of the diffusion coefficients for the plasma with N-ITB (solid line) and without N-ITB (dashed line).

The impurity flux is expressed as $\Gamma = -D(\partial n_z / \partial r) - n_z V$, where D and V are coefficients for the diffusive and convective term, respectively. Because the electron density profile is almost flat during ECH as shown in Figure 2 (c), we assume that convective velocity can be neglected (V=0). The results of the calculation are shown in Figure 6 (b). The average energy of the titanium K_α lines is plotted as a function of the impurity diffusion coefficients $D_{in.}$. The solid line denotes the dependence for the plasma with N-ITB, and the dashed line denotes that for the plasma without N-ITB. The core diffusion coefficient is reduced to <0.02 m²/s in the plasma with N-ITB, while it is 0.1-0.18 m²/s in the plasma without N-ITB. In the N-ITB discharge, because the transport time scale is comparable to the atomic process time (the ionization and the recombination), the averaged Ti $K\alpha$ line energy is sufficiently sensitive to the impurity diffusion.

6. Radial Electric Field in EC Heated NBI Plasma with N-ITB

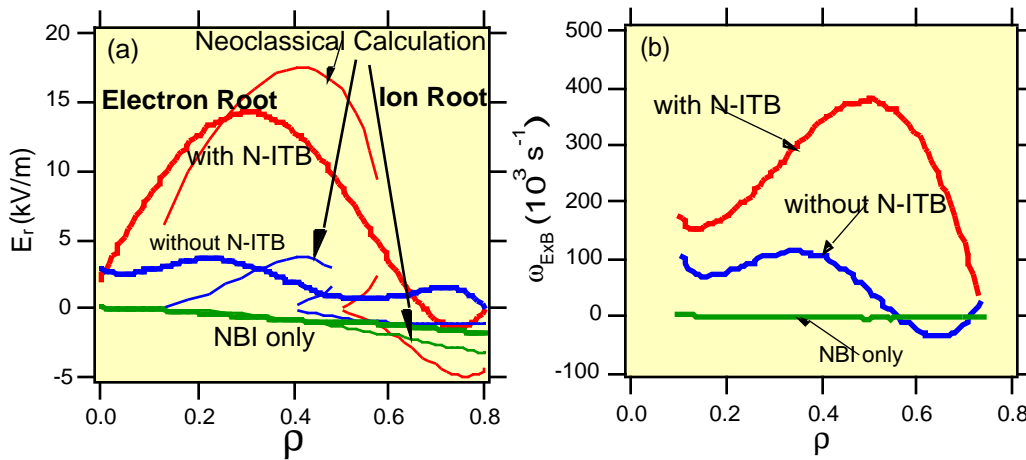It is also confirmed with the HIBP measurement that this transport barrier is accompanied with

Figure 7. (a) Profiles of the radial electric field and (b) ExB shearing rate. The thick and the thin lines denote the experimental and the neoclassical estimation. The red and the blue lines denote the plasma with N-ITB and without N-ITB, respectively. The green line denotes the NBI plasma without ECH.

the large positive radial electric field ($E_r \sim 15$kV/m), as shown in Figure 7(a). On the other hand, the plasma without N-ITB has smaller E_r (Er<5kV/m) and the NBI plasma without ECH has negative E_r. Figure 7 (a) also shows profiles of the neoclassical estimation of radial electric field that is derived from the ambipolar condition for those three cases. These theoretical curves qualitatively support the experimental observations. It is clear that the radial electric field of N-ITB is induced by the transition from the ion to the electron root.

The ExB shearing rate [9] ($\omega_{EXB} = RB_\theta{}^2/B(\partial/\partial y)E_r/RB_\theta$) is plotted in Figure 7 (b). Here, R is the major radius, B_θ is the poloidal magnetic field, B is the magnitude of the magnetic field, E_r is the radial electric field and ψ is the flux coordinate. The ExB shearing rate ($\omega_{ExB} \sim 1 \times 10^5$ s^{-1}) in the plasma without N-ITB is smaller. In NBI plasma without ECH, the sharing rate ($\omega_{ExB} \sim -0.4 \times 10^3 \, s^{-1}$) is negligible compared to plasma with ECH. The maximum shearing rate ($\omega_{ExB} \sim 4 \times 10^5 s^{-1}$, $dEr/dr \sim 300$kV/m^2) is comparable to that at the internal transport barrier observed in Tokamak experiment.

7. Estimation of Thermal Diffusivity for N-ITB Plasma and Discussions

In the previous N-ITB experiment with ECH, the improvement of the ion thermal transport was not identified. This is because the transferred energy to ions from electrons is small for low collision frequency in the high electron temperature. In EC heated NBI plasma, on the other hand, the more electron temperature increase, the larger contribution to the ion heating is given from NBI. We estimate NBI power deposition with MCNBI code, which is based on the Monte Carlo simulation [10]. According to the MCNBI code calculation, the fraction for the ion heating of the deposited NBI power is greater than ~50%, when the electron temperature is higher than ~1keV on CHS, as shown in Figure 8 (c). In this calculation, the acceleration voltage is 36kV, the beam current is ~40A, the port through NBI power is ~700kW, and the density is 3.5×10^{12}cm^{-3}.

There is a problem whether the increase in the electron and ion temperature is due to the improvement of the confinement or due to the increase in the deposition power of NBI. To make sure of this, the calculation of the power deposition is carried out with MCNBI code for the N-ITB plasma (Fig. 8 (a)) and the plasma without N-ITB (Fig. 8 (b)). Total deposited power is 37 kW for Fig.8 (a) and 60kW for Fig.8 (b). The calculation uses the real geometry and orbit averaging is made. But the finite orbit effect during slowing down processes is not calculated and electric field is not included.

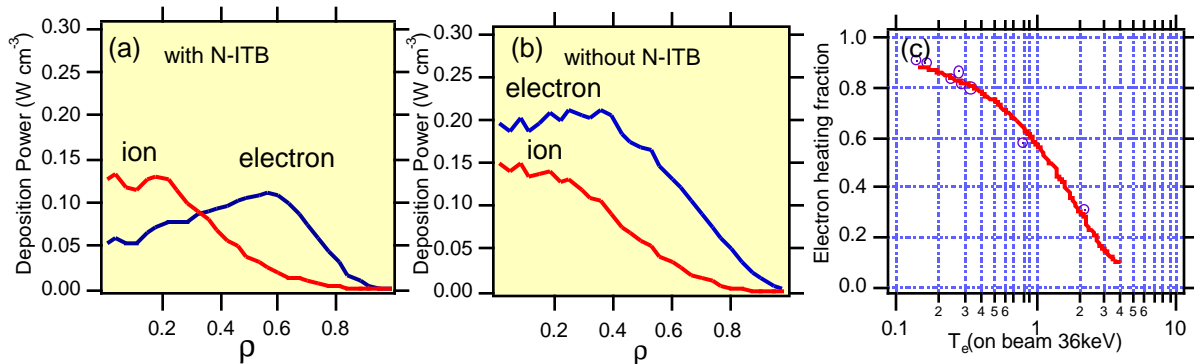First, we consider difference of power deposition to electrons in the plasmas with N-ITB and

Figure 8. NBI power deposition profile to electrons and ions for the plasma with N-ITB (a) and without N-ITB (b).
(c) Electron heating fraction of NBI deposition as a function of the electron temperature.

without N-ITB. ECH power deposition rate is estimated larger than 90% for both cases (see below). The total deposited NBI power to electrons in the plasma with N-ITB is about 55% compared to the plasma without N-ITB. Consequently, electron heating power is smaller for N-ITB plasma and the large increase of the central temperature is not explained by the change of heating power. This conclusion is supported by the results of the N-ITB ECH experiments which provide the similar results [1] . Secondly, for the power deposition to ions, Fig. 8 (a) and (b) give almost the same level heating power. Although the density of N-ITB plasma is slightly lower for N- ITB plasma, large increase of ion temperature (two to three times higher) is not explained by the difference of heating power.

In order to analyze confinement properties N-ITB plasma. We calculated thermal diffusivity using plasma profile data in Fig. 3 and power deposition profile in Fig. 8.

The transport analysis is carried out to clarify the characteristic of the N-ITB. In the steady state, the heat conductions $Q_{cond}^{electron}, Q_{cond}^{ion}$ are expressed as follows.

$$Q_{cond}^{electron} = \frac{3}{2}\nabla(T_e\Gamma_e) - 3\frac{m_e}{m_p}\frac{n_e}{\tau_e}[Z](T_e - T_i) + Q_{ech} + Q_{NBI}^{electron} \tag{1}$$

$$Q_{cond}^{ion} = \frac{3}{2}\nabla(T_i\Gamma_i) - 3\frac{m_e}{m_p}\frac{n_e}{\tau_e}[Z](T_i - T_e) + Q_{NBI}^{ion} \tag{2}$$

Here Γ_e and Γ_i are the radial particle fluxes of the electron and ion ,respectively. m_p, m_e indicate electron and ion mass, respectively, τ_e is electron collision time. These values are estimated using the Proctr-MOD code [11]. Q_{ech} is for ECH. ECH absorbed power is derived by the formula using I. Fidone and G. Granata [12]. In the plasma with low density and high electron temperature plasma, all injected power ($P_{inj}\sim$ 130kW) reaches the resonance zone and over 90% power is absorbed when the electron temperature is above 1 keV. The χ_e and χ_i is defined as $\chi_e = Q_{cond}^{electron}/n_e\Delta T_e, \chi_i = Q_{cond}^{ion}/n_e\Delta T_i$.

Figure 9 shows electron ion diffusivity for two plasma discharges with N-ITB (in red) and without N-ITB (in blue). Error bar for the experimental diffusivity reflect error bars in the profile measurement. Figure 9 also shows neoclassical transport coefficients evaluated with the analytical formulae derived by Kovrizhnykh [13,14] . Due to the nonlinear dependence of the neoclassical particle fluxes on the radial electric fields (E$_r$), the E$_r$ and the fluxes are determined by the
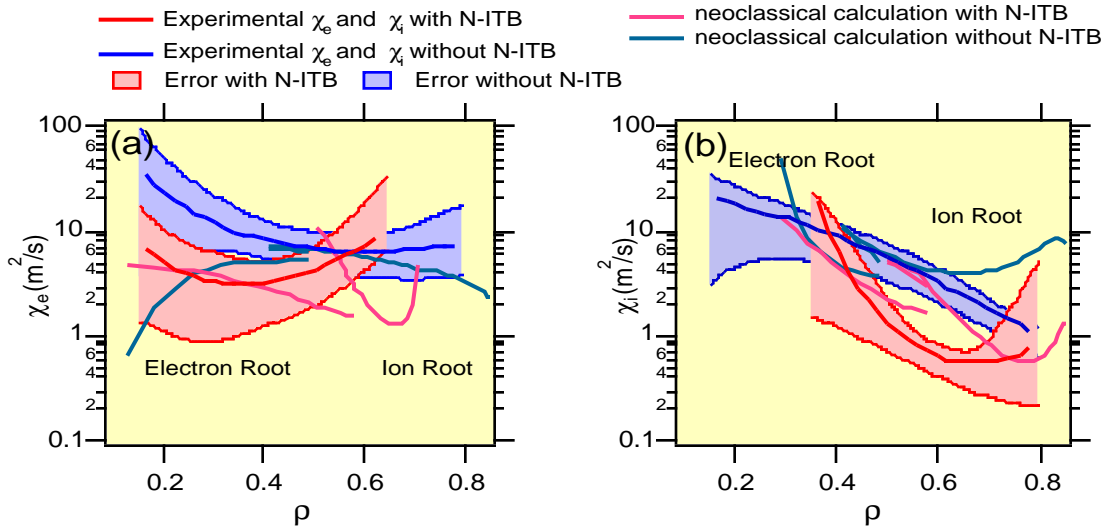

Figure 9. Comparison between experimental thermal diffusivity with N-ITB and without N-ITB for the electrons (a) and teh ions (b). The dashed lines denote the neoclassical estimation.

ambipolar condition($\Gamma_e(E_r)=\Gamma_i(E_r)$) calculated from T_e,T_i and n_e.

For the electron thermal diffusivity, the N-ITB plasma gives reduced χ_e at $\rho\sim0.3$ compared to plasma with N-ITB. It is main reason for the electron temperature increase of core region. For ion diffusivity ,the present transport analysis shows the χ_i reduction at $\rho\sim0.6$ for N-ITB plasma which is the direct reflection of the steep ion temperature gradient at that position. Although further study is necessary to make final conclusion and more complete understanding, this results suggest the formation of the ion thermal transport barrier in the new N-ITB plasma.

8. Summary

(1) New N-ITB regimes are found with the improved confinement for both ions and electrons in EC heated NBI plasmas.

(2) The improved confinement region is expanded for electrons from $\rho_f\sim0.3$ to $\rho_f\sim0.4$ compared to previous N-ITB experiments.

(3) With N-ITB formation, the ion temperature increases by about two to three times. The ion temperature gradient also increases at $\rho\sim0.6$. The present transport analysis suggests the formation of ion thermal transport barrier.

(4) The decrease of the ion temperature is much slower than that of the electron temperature after the electron transport barrier disappears.

(5) The large E_r and E_r shear are observed.

(6) The impurity transport is decreased inside the barrier.

(7) Further investigation should be made to understand (a) whether the mechanism of the confinement improvement for electrons and ions are different or the same, (b) the difference of foot point locations for electrons and ions, (c) the relation between confinement improvement and the electric field structure.

Acknowledgement

References
[1] Minami, T., et. al.,Plasma Phys. Control. Fusion **44** (2002) 197
[2] Fujisawa, A.,.et.al. Phys.Rev.Lett **82** (1999) 2669
[3] Minami, T., et. al., J.Plasma Fusion Res. SERIES, **4** (2001) 451
[4] Narihara, K., et.al., Rev.Sci.Instrum. **66** (9) (1995)
[5] Ida, K., et.al. Rev. Sci. Instrum. **60** (1989) 867
[6] Liang, Y., et.al. Phys. of Plasmas **9** (10) (2002) 4179
[7] Ida, K., et.al. Nucl. Fusion **39** (1999) 1649
[8] Minami, T., et. al., (proc. 26th EPS Conference Maastricht 1999) P3.109 p1357
[9] Burrell, K.H.Phys., Plasmas **4** (5) (1997) 1499
[10] Murakami,S., et.al.,J. Plasma Fusion Res. SERIES, **2** (1999) 255.
[11] Howe, H, C.,. Rep. ORNL/TM-11521, TN(1990)
[12] Fidone,I. and Granata,G., Nucl. Fusion **11** (1971) 133
[13] Yokoyama,M., et.al., Nucl.Fusion **42** (2002) 133
[14] Kovrizhnykh,L.M., Nucl. Fusion **24** (1984) 435